



Bulletin of the Mineral Research and Exploration

<http://bulletin.mta.gov.tr>



An ore adit planning with the help of three dimensional ore body modeling: A case study from Çulfa Çukuru Pb-Zn-Cu-Ag deposit

Sinan AKISKA^a and Elif AKISKA^{b*}

^aAnkara Üniversitesi Mühendislik Fakültesi Jeoloji Mühendisliği Bölümü, 06830, Gölbaşı, Ankara. orcid.org/0000-0001-8262-7349

^bAnkara Üniversitesi Mühendislik Fakültesi Jeoloji Mühendisliği Bölümü, 06830, Gölbaşı, Ankara. orcid.org/0000-0002-6180-4710

Research Article

Keywords:

Modeling, geostatistics, ore, kriging, idw.

ABSTRACT

Çulfa Çukuru Pb-Zn-Cu-Ag mineralization has occurred along the metamorphic and metamorphic-dacitic volcanic rock contacts of the Sakarya zone on the Biga Peninsula. The base metal mineralizations ($Pb-Zn-Cu-Ag \pm Au$) developed along the contact and fracture planes of these rocks can be observed as veins, lenses and disseminated ore geometries in the calc-silicate rock assemblages. Base metal mineralizations are mainly controlled lithologically and are generally associated with recrystallized limestones. In this study, the surface and the subsurface were modeled using the topographical data and the geochemical data (Pb% and Zn%) collected from 42 boreholes of Çulfa Çukuru which is located 20 km South-Southeast of Kalkım (Çanakkale). The surface and the subsurface data were interpolated by Kriging and Inverse Distance Weighted methods, respectively. The intersectional areas of Pb% and Zn% modeling data obtained from this study were determined by dividing the areas above the cut-off grade into 4 different sectors (low, intermediate, high, and very high). Using the distribution of the intersections of these sectors, the possible adit lines were determined and also an interpreted map of the adit was drawn for 450 level. This modeling study helps to plan the ore adit to be opened in a mining area. Moreover, according to the important changes that may occur in conditions (e.g. fluctuations in metal prices or decreasing-increasing costs), models can also be modified during operations.

Received Date: 26.05.2017
Accepted Date: 11.02.2018

1. Introduction

One of the most problematic issues encountered during the assessment of mineral deposits is that we do not have any observations for the entire subsurface. However, the data obtained from boreholes, well logs, and by geophysical methods can provide us some important information about underground. The use of the borehole data for the interpretation can only be achieved by combining this data with appropriate interpolation methods. That is why, the choice of an appropriate interpolation method is very important for the most accurate estimate to the real values. Using the estimation error values and the cross-validation data, the accuracy of the applied interpolation method can be checked.

With the development of computer technology, the utilization of 3D (3-dimensional) modeling of

complex structures has increased considerably over the last few decades. A large amount of data can now be evaluated and interpreted together with the help of computers capable of high level processing. With the support of these studies, many problems that we encounter in during the actual work can be solved. In the geosciences, modeling studies are used frequently in the detection of subsurface location and the evaluation of natural resources such as ore deposits (Saraç and Tercan, 1996; Chen et al., 2007; Feltrin et al., 2009; Wang et al., 2011; Liu et al., 2012; Wang and Huang, 2012; Xiao et al., 2012; Akiska et al., 2013; Kashani et al., 2016), oil, natural gas and coal (Sims, 1992; Saraç et al., 2004; Kaufmann and Martin, 2008; Jian et al., 2012; Dağ and Özdemir, 2013), hydrology and hydrogeology studies (Turner, 1992; Watt et al., 2007; Ahmed, 2009; Gallerini and Donatis, 2009), determining structural elements (Renard and Courrioux 1994; de Kemp, 2000; Galera et al., 2003;

* Corresponding author: Elif AKISKA, egunen@eng.ankara.edu.tr
<http://dx.doi.org/10.19111/bulletinofmre.372510>

Bistacchi et al., 2008; Calcagno et al., 2008; Zanchi et al., 2009; Dhont et al., 2012), and solving road, tunnel and dam problems (Veldkamp et al., 2001; Elkadi and Huisman, 2002; Rengers et al., 2002; Özmutlu and Hack 2003; Zhu et al., 2003; Hack et al., 2006; Choi et al., 2009).

In this study, using the data from the geochemical analyses obtained from the 42 boreholes in Çulfa Çukuru Pb-Zn-Cu-Ag mineralization, the 3D subsurface modeling were made. The areas above the cut-off grade were determined and the optimal adit lines were detected using these models. These modeling studies were controlled by statistical and cross-validation techniques. The appropriate parameters can be determined by interpreting the geological, structural, and economic conditions of the deposit and using these parameters, it is possible to detect how to extract the ore from the underground in an optimal way by making a model both before and during an underground operation.

2. Regional Geology

Based on the geological studies of Biga Peninsula (Siyako et al., 1989; Okay et al., 1990, 1996, 2008; Dönmez et al., 2005, 2008; Altunkaynak and Genç 2008; Dilek et al., 2009), the basement of the area consists of Paleozoic-Mesozoic metamorphic rocks and ophiolitic rocks. The area was affected by intense magmatism from Paleocene to the end of Miocene. During this period, while many granodiorite bodies, mostly composed of granodiorite, intruded into the basement rock, these were covered with andesitic-dacitic-rhyodacitic-rhyolitic volcanic rocks unconformably. Also during this period, volcanic activity on the Biga Peninsula was often accompanied by an intense sedimentation. The last volcanic products in the area are represented by Pliocene basalts. All of the units were unconformably covered by the Plio-Quaternary fluvial units (Figure 1a).

Based on detailed studies of the Çulfa Çukuru area by Akısla (2010), Akısla et al. (2010, 2013), Akısla and Demirela (2014), the units, from older to younger, are Çamlık granodiorite (Devonian), Permo-Triassic Kalabak metamorphic rocks, including metasandstone and calc-schist lenses (Permo-Triassic), Eybek pluton (Oligo-Miocene), and Kalkım volcanics (Middle Miocene) (Akısla, 2010).

Çamlık granitoid was investigated by Okay (1990), and the ore geology of Çulfa Çukuru area was

studied by Yücelay (1976), Çetinkaya et al. (1983a, b), Tufan (1993). The researchers have mentioned the existence of tectonic contact between this unit and Kalabak schist. This unit includes quartz, plagioclase, and chlorite with grey-brown color macroscopically and is cut by aplite and quartz veins (Akısla, 2010).

The Kalabak Formation was first described by Radelli (1970) as "Kalabak schists". This formation overlays the lithological units of Precambrian Kazdağ massif with angular unconformity outside of the study area and is overlain with Çamlık granitoid in the south of the study area. This formation is also covered by Kalkım volcanics and Akköy Formation with angular unconformity in the North (Tufan, 1993). According to Yücelay (1976), Çetinkaya et al. (1983a, b), Tufan (1993), The Kalabak Formation includes clayey schist, biotite schist, sericite-chlorite schist and sericite-graphite schist with metasandstone, marble, serpentinite, and meta-diabases lenses (Akısla, 2010).

Eybek pluton (Tufan (1993), Andıç and Kayhan (1996), Pehlivan and Çetin (1997), and Genç and Altunkaynak (2007) is mainly composed of granite, quartz monzonite and granodiorite. The main minerals in the rocks are quartz, alkali feldspar, plagioclase (generally albite-andesine type), biotite, hornblende and augite, while the accessory minerals are titanite, zircon, apatite and opaque minerals (Akısla, 2010).

Kalkım volcanics (Yücelay (1976), Çetinkaya et al. (1983a, b), Tufan (1993), Andıç and Kayhan (1996), and Pehlivan and Çetin (1997) were correlated with the Hallaçlar Formation by Krushensky (1976) (Akısla, 2010). They are represented by rhyolite, dacite, andesite, trachyandesite, ignimbrite, tuff, and agglomerates (Figure 1a, b) (Akısla, 2010).

Çulfa Çukuru Pb-Zn-Cu-Ag mineralization is observed to be related to the metamorphic rocks and volcanic rocks belonging to the Sakarya zone in the Biga Peninsula. The base metal mineralizations at the contact between these rocks and along the cracks and fault planes are seen as veins, lenses and disseminations in the calcsilicate rock assemblages. Although the relationship between the mineralization and wall rock is seen between volcanic and metamorphic rock, the direct relationship of the volcanic rock with mineralizations is not well proven. Base metal mineralizations are mainly controlled by lithology and are generally associated with recrystallized limestone (Figure 1a, b).

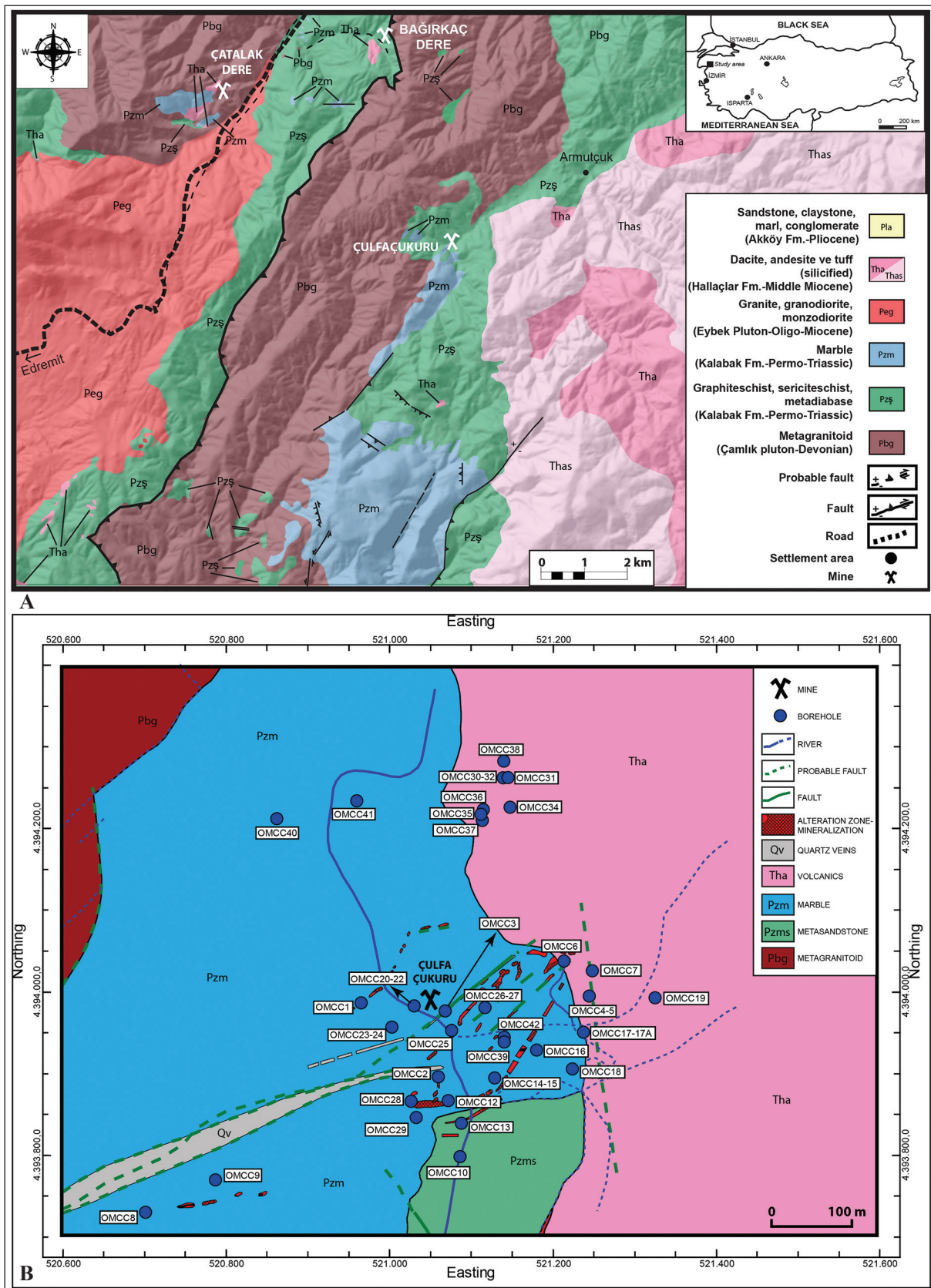


Figure 1- A) Geological map of the Çulfa Çukuru area and its surroundings (modified from Duru et al., 2007), B) Geological map (Yücelay, 1975) and the borehole locations of the Çulfa Çukuru Pb-Zn deposit (the coordinates are given in UTM coordinate system – 35N).

3. Methods

3D underground modeling studies have, in recent years, been accelerated with the development of computer technology. The complex studies can be done easily with computers. As a result, there has been a rapid increase in modeling studies, and subsurface ore modeling has become one of the most frequently used. The accurate estimation of the ore in an underground environment minimizes expenditure for mining companies, the correct orientation of the adit direction in underground mining areas playing the most important role in this cost reduction.

In earth sciences, interpolation is used for both prediction and visualization (Falivene et al., 2010). A number of algorithm have been developed to perform interpolation such as; kriging (Krige, 1951; Matheron, 1960), splines (Ahlberg et al., 1967; Mitasova and Mitas, 1993), inverse distance weighting (IDW) (Kane et al., 1982) and polynomial regression (Wang and Huang, 2012). In many cases, the kriging method is the best predictor, while in some cases IDW and spline are considered more suitable methods (Zimmerman et al., 1999; Peralvo, 2004; Chaplot et al., 2006; Binh and Thuy 2008; Shahbeik et al., (2014). In order to determine the ore distribution correctly, it is important

to choose the best estimation method and thus minimizing the estimation errors.

In this study, the surface and subsurface modeling were performed using topographic data and geochemical data of Pb-Zn deposit in the Çulfa Çukuru area, respectively, and the direction of the adits to be opened underground was determined with the help of mathematical operations. The data set which was created for this study consists of topographic, borehole and geological data. For the interpolation method, Ordinary Kriging (OK) method was used and for surface modeling and IDW method were used for subsurface modeling in this study (Figure 2).

Kriging is a statistical interpolation method used to determine unknown points from the points in a data set, and is the usual name of generalized least squares regression algorithms (Cressie, 1990; Li and Heap, 2008). This algorithm is an estimation method used to detect unknown values with the help of known values and semi-variograms. The distinction from most other methods is the use of spatial continuity among the data (Wang and Huang, 2012). It also minimizes the variances among the estimations and makes the estimate in the most appropriate way at each unknown point. Kriging variance depends not

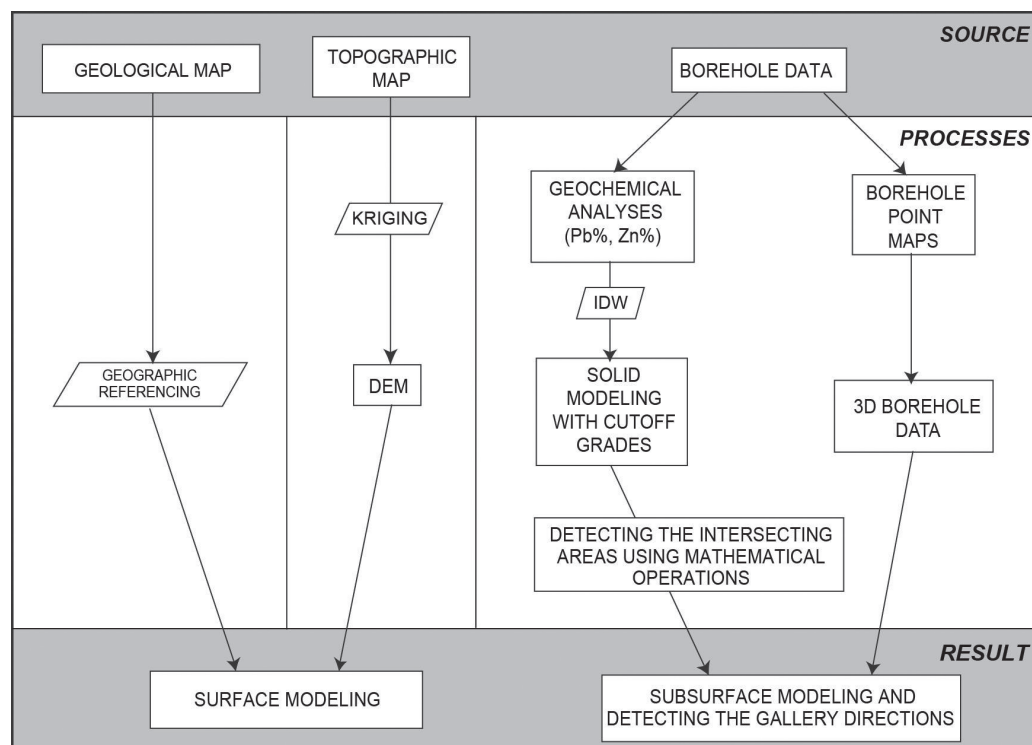


Figure 2- Flow chart of the modeling processes.

on the real values of the data, but on a function of the amount of data and the distances between the data collection points. The most important advantage of this method is the weights determined with the help of certain mathematical operations. The data is analyzed systematically and the weights are decided using semi-variograms. The availability of Kriging depends on the compatibility of the selected semi-variogram. Semi-variogram (experimental semi-variogram) is a graphic used in applied geostatistics for determining the spatial dependencies among the data (Kitanidis, 1997). A semi-variogram is calculated from the mean of all the specified separation distances and directions and half of the squared difference of z-values over all observed pairs (Wang and Huang, 2012). The accuracy rate of the data produced by the Kriging method depends on the amount of data, the frequency of the data and the accuracy of the semi-variogram (Brooker, 1986; Chaouai and Fytas, 1991). There are different Kriging techniques, OK is one of the most commonly used. The estimation of unknown values in the OK method is realized according to the assumption of the unknown-constant mean and the stationary variables. In addition, OK is a linear model based on local neighborhood structure (Tahmasebi and Hezerkani, 2010).

The IDW method uses the weights obtained from the produced inverse function depending on the distance between the sampled points and unsampled points (Li and Heap, 2008). The sampled points closer to the unsampled points are given more weight, and vice versa. According to the assumption of this method, the values belonging to unsampled points are more similar to the closer points than the farther points. IDW is a sensitive method and gives extremely accurate results for a wide range of data interpretations (Lam, 1983). The basic factor affecting the accuracy of the IDW method is the power parameter (p) in the formula. The weight decreases as the distance increases. When p value increases, the closer points get more weight and the resulting spatial interpolation is local (Isaaks and Srivastava, 1989). The most important feature of this method is that it can interpolate dispersed data in regular grids or irregularly spaced data very quickly (Li and Heap, 2008). Although the application of this method is easy, "bull's-eye" patterns can also be seen due to the concentric contours created by the IDW method (Burrough and McDonnell, 1998; Van Dijk et al., 1999; Dressler, 2009).

The neighborhood estimation is very important in terms of limiting the data used (Johnston et al., 2001).

It is created by drawing a circle or ellipse around the estimated point. The values within these are then considered, while the ones outside are not taken into account (Fencík and Vajsálová, 2006). In addition, to prevent trending in a certain direction, the circle or ellipse can be divided into sectors.

In surface modeling studies, DEM is created with the help of topographic data and a 3D surface map obtained. DEM is created by the determination of unknown values from known values with the help of interpolation methods. The IDW method is applied to the subsurface modeling. Through this method, the intersecting areas of Pb% and Zn% values above the cut-off grade were detected. The basic logic for this method is to determine the area with most potential for ore being found in the underground environment. This method of intersecting areas was applied by Akiska et al. (2013) to determine the potential ore areas in an underground environment. The study was checked both with cross-validation methods and in the field survey, the results were highly promising.

Cross-validation is a process which tests whether a study is consistent with its goals (Olea, 1999). Cross-validation is the most common method used to control the accuracy of an interpolation method (Voltz and Webster, 1990). It is a method of testing the reliability of a selected model by estimating the values at the sample points with the help of neighborhood values and comparing the predicted values using measured values (Davis, 1987). According to this method, a known value is removed from the dataset temporarily and the value of this point is estimated with the help of neighborhood data. Thus, the error between the measured value and estimated value can be observed. This process is repeated for all remaining samples (Isaaks and Srivastava, 1989). Cross-validation is very important for getting rid of unnecessary data redundancy (Olea, 1999; Webster and Oliver, 2001), and all the data obtained can be used for prediction. This method can also be used for selecting the best variogram model among the possible models and to select the lag size, also to search radius in order to minimize the kriging variance (Davis, 1987; Olea, 1999). In addition, this method helps in finding the best parameters from the test data for IDW and spline methods (Robinson and Metternicht, 2006).

Some prediction errors are used in this study. These are Mean Error (ME), Root-Mean-Square Error (RMSE), Mean Standardized Error (MSE), Root-Mean-Square Standardized Error (RMSSE), and

Average Standard Error (ASE) for surface data, Mean Error (ME) and Root-Mean-Square Error (RMSE) for subsurface data and Coefficient of Determination (R^2) for both data sets.

4. Results

4.1. Geostatistical Analysis of the Surface Data

The study area is located 13 km south of Kalkım (Çanakkale) and covers 0.7 km^2 ($1000 \text{ m} \times 700 \text{ m}$). The topographic data was digitized from Yücelay (1975) and the information about the survey method was not given in the study. The distance between contour lines is 10 meters. The scale of the topographic map is 1:2000. The total number of x, y and z values is 8502. The heights are generally irregularly distributed (non-flat topography), the minimum height is 450 meters and the maximum height is 670 meters. The mean height is 547.16 meter and standard deviation

is 55.824. The surface was divided into $2 \times 2 \times 5 \text{ m}$ blocks (2450000 total voxels) for the modeling study.

In this study, the experimental semi-variograms were calculated in four different directions (N-S, E-W, NE-SW and NW-SE) no directional effects were observed for semi-variograms. Both the sill and range values were almost the same in the variograms calculated in all four directions. Lag size of the semi-variogram is 52.72 m and “Spherical Model” provided the best fit for the experimental semi-variogram. The range value is 517.52 m, the sill value is 5396.57 m and the nugget value is 0 m. (Figure 3a).

In this study, the neighborhood shape was selected as a circle because of the absence of any directional effects within the spatial autocorrelation of the data. The circle was divided into 4 sectors with 45° offset. The number of neighbors was between 2 and 5.

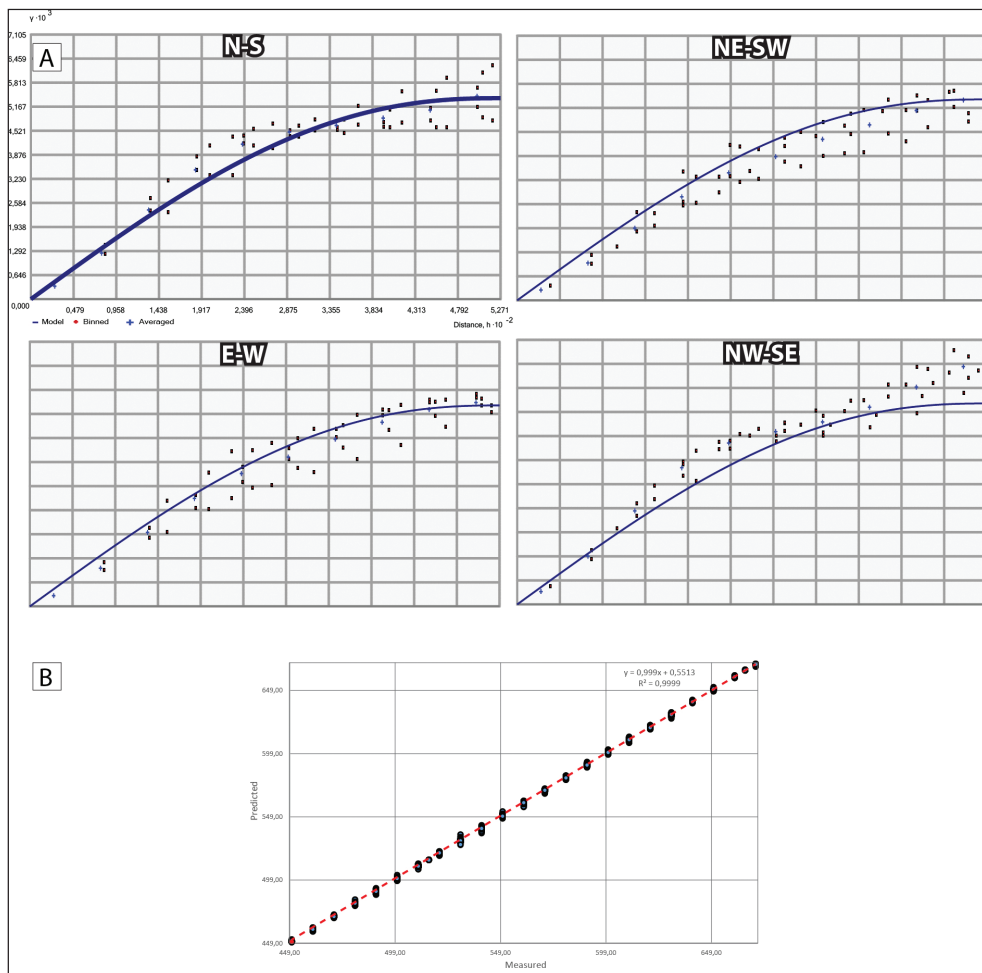


Figure 3- a. Generated experimental semi-variograms according to the directions, b. The scatter plot of the measured-predicted values of surface data.

The accuracy of surface values in this study was tested using cross-validation method (Figure 3b) and ME, RMS, ASE, MSE, and RMSS prediction errors were used to compare the models. The cross-validation method was used on all of the data (8502 points). The prediction errors in this study are 0.25 for ME, 0.52 for RMSE, 0.006 for MSE, 0.09 for RMSE and 6.22 for ASE (Table 1). To ensure that the created DEM is as accurate as possible; ME and MSE should be close to 0, RMS should have the lowest value, ASE should be close to RMS value, and RMSS value should be close to 1 (Johnston et al., 2001; Webster and Oliver, 2001; Hu et al., 2004). The results obtained from the cross-validation technique and prediction errors

Table 1- Surface modeling prediction errors of Çulfa Çukuru area.

Samples	n	8502
Mean Error	ME	0.02485
Root-Mean-Square Error	RMSE	0.51497
Mean Standardized Error	MSE	0.00617
Root-Mean-Square Standardized Error	RMSSE	0.08534
Average Standard Error	ASE	6.21714

indicate that the prediction values similar to real values are produced as possible. The cross-validation diagram is shown in figure 3b and the prediction errors are seen in table 1. The created 3D surface map using topographic values is also shown in figure 4.

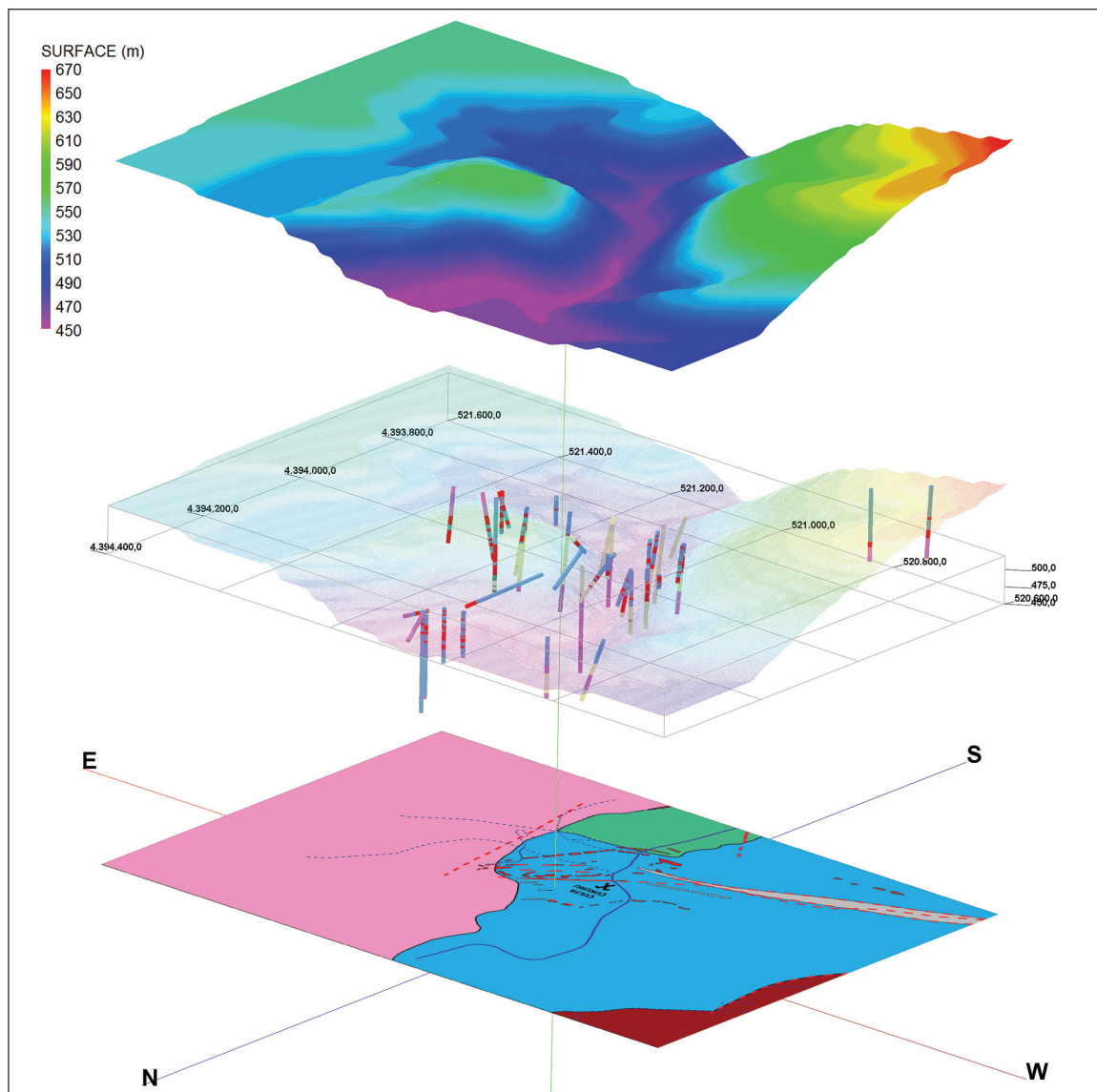


Figure 4- 3D topographic map, boreholes, and geology map of Çulfa Çukuru Pb-Zn deposit (to avoid confusion, +1000 m. offset and -1000 m offset along z axis were applied on geology map and topographic map, respectively) (see Figure 1 for the legend of geological units).

4.2. Three-Dimensional Subsurface Modeling of Mineralization

The study area is located in a 0.7 km² area and has an irregular topography. In the study area where both flat areas and hills are located, Akpinar stream flows from north to south. The main mineralization in the area was discovered in this stream bed, and then subsurface continuity of the mineralization was found in more detailed studies (Figure 4).

The block model with IDW algorithm was applied to Pb% and Zn%. The values obtained from the geochemical analyses on the ore-alteration zones with a total of 42 boreholes were used for the Pb% and Zn% values. The shallowest drilling is 19.5 m (OMCC1) and the deepest drilling is 161.5 m (OMCC37). The total depth of drillings is 3622.4 m and average depth of drillings is 86.25 m. The ore-alteration zones were observed 7 out of 42 boreholes (OMCC10, OMCC24, OMCC26, OMCC38, OMCC39, OMCC40, and OMCC41) (Figure 4). Using Pb% and Zn% geochemical analyses values, the individual model files were created for each element percentage with the help of the IDW interpolation method. The data was modeled using cut-off grades, 7% for Pb and 4% for Zn and 2637765 voxels which were 2 x 2 x 5 m in dimension.

Inverse distance, using constant or variable exponential weighting, assigns a voxel node value based on the weighted average of neighboring data points. In this study, the sector shape is circular because there was no directional effect on the regional autocorrelation in the data and the factor of anisotropy

is 1. The power and the number of neighborhood values were tested and the optimal values are; power value 8, neighborhoods 6 for Pb%, power value 4, neighborhoods 2 for Zn%.

The distribution of the ore zones that was followed during the modeling studies, using geochemical analysis data for each element, covers quite large areas in the subsurface environment (Figure 5). It seems quite difficult to determine the target area in this way. Therefore, for both Pb% and Zn%, the values above the cut-off grade are divided into four equal sectors. These sectors are referred to as "Low", "Intermediate", "High", and "Very High" (Table 2). The ore zones which were created separately for each sector can also be observed in a wide range area. This is a common situation especially when the amount of data is limited (e.g. insufficient number of boreholes, irregularly spaced boreholes etc.). This is why, instead of evaluating the data of each sector separately, using the intersection of the sectors in the same category seems to be more suitable at detecting target area (e.g. the intersection of the "low" grading sector of Pb% and the "low" grading of Zn%). Although it is possible to find the ore zones outside of these areas, the promising areas are the intersectional areas (Akiska et al., 2013).

In order to create intersection areas, the first created model files are converted to Boolean model files. When the intersection areas are detected, the corner coordinate values of each cube are detected and it is also determined whether the values contained herein are within the given range. In these Boolean model files, 1 is assigned to the values in the given intervals and 0 is assigned to the remaining values.

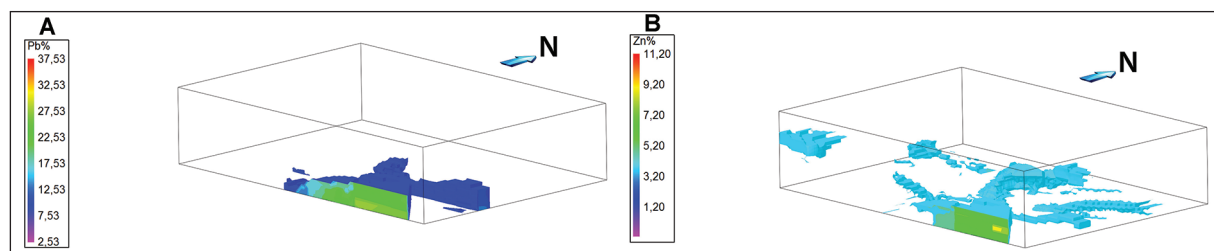


Figure 5- Areas of Pb% (a) and Zn% (b) values above the cut-off grade in the subsurface environment.

Table 2- Sector names and properties using in subsurface modeling study.

Sector #	Sector Name	Pb% Intervals	Zn% Intervals	Pb% Boolean Model File	Zn% Boolean Model File
1	Low	7.00–14.81	4–6.33	Pb_bool_sector1	Zn_bool_sector1
2	Intermediate	14.81–22.62	6.33–8.66	Pb_bool_sector2	Zn_bool_sector2
3	High	22.62–30.43	8.66–10.98	Pb_bool_sector3	Zn_bool_sector3
4	Very High	30.43–38.24	10.98–13.31	Pb_bool_sector4	Zn_bool_sector4

The generated Boolean model files are then transferred to MS Excel. With the help of a macro written in MS Excel, the “1” values (ore grade values in the specified range) were taken into account while “0” values were excluded from the modeling study.

The Boolean files for each sector (“low”, “intermediate”, “high”, and “very high”) and each element were created using the method described above. Then, in order to detect the intersection areas of each sector, multiplication was applied to the Boolean model files (e.g., the values in Pb_bool_sector1.mod and Zn_bool_sector1.mod were multiplied by each other to find the intersection areas of Sector1) (Figure 6). The process of detection for the intersecting areas was applied to every sector, and these areas were determined. Details and applications of this method were given in Akıška et al. (2013).

In the region with the obtained data; a mass of ore with a total volume of 1100000 m³ including 382000 m³ for Sector1, 696000 m³ for Sector2 and 22000 m³ for Sector3, was identified. Since the 0 value is obtained by multiplying the Boolean files belonging to Sector 4, referred to as “Very High”, the result is that there is no intersected area between these ranges (Figure 7).

Attempted detection of the adit directions and locations was done using sector values that were obtained using the intersection method. When the adit locations were detected, the elevation intervals of the adits were randomly determined as being 10 meters (450-520 levels) and the adit dimensions as 2 x 2 meters. These intervals can be increased, decreased or changed according to the subsurface environment conditions and lithological conditions during adit planning. The related sectors for each level were brought together and the adit line of that level was

created. In addition, it was determined which sector will be seen in which location on a certain level (Figure 8).

The case study for 450 level was made. The top view and the side view of the adit line including all sectors in the 450 level are seen in figure 9a and 9b, respectively. Each point on the level shown in Figure 9b implies the area where the ore is located. The interpreted map using Figure 9a and 9b was drawn for 450 level (Figure 9c). The strike of the first entrance is N105E. The general trend of the adit is E-SE. In the interpreted map, the location of the adit entrance and the general orientation of the adit were determined from the model image (Figure 9a). It was checked with the topographic map whether this point (adit entrance) coincided with a point on the surface. The detected point may not be exactly on the surface, but on the subsurface. This is because the points in the model file are due to the presence of ore in the specified intervals in the sectors. If the point determined as the entrance of the adit does not contain ore at these intervals, the point containing the ore closest to the surface can be detected and the entrance of the adit can be determined accordingly. Likewise, these maps can be created for all levels so that adit planning can be done.

The accuracy of the subsurface modeling studies was checked statistically and using cross-validation techniques. The estimation errors and cross-validation graphic can be seen in figure 10 and table 3, respectively. The cross-validation technique is applied to all the data used in the interpolation creation (7170 points). The fact that the R² values are close to 1, the Mean Error values are very close to 0, and the RMS values are relatively low values, they indicate that the applied interpolation algorithm and related parameters were selected very closely to the real values.

<table border="1" style="border-collapse: collapse; width: 100%; height: 100%;"> <tr><td>0</td><td>1</td><td>1</td><td>0</td><td>0</td></tr> <tr><td>0</td><td>1</td><td>1</td><td>1</td><td>0</td></tr> <tr><td>0</td><td>1</td><td>1</td><td>1</td><td>1</td></tr> <tr><td>1</td><td>1</td><td>1</td><td>0</td><td>0</td></tr> <tr><td>0</td><td>0</td><td>0</td><td>0</td><td>0</td></tr> </table>	0	1	1	0	0	0	1	1	1	0	0	1	1	1	1	1	1	1	0	0	0	0	0	0	0	x	<table border="1" style="border-collapse: collapse; width: 100%; height: 100%;"> <tr><td>0</td><td>0</td><td>1</td><td>1</td><td>0</td></tr> <tr><td>0</td><td>1</td><td>1</td><td>1</td><td>0</td></tr> <tr><td>0</td><td>1</td><td>1</td><td>1</td><td>1</td></tr> <tr><td>0</td><td>1</td><td>1</td><td>1</td><td>1</td></tr> <tr><td>0</td><td>0</td><td>1</td><td>1</td><td>1</td></tr> </table>	0	0	1	1	0	0	1	1	1	0	0	1	1	1	1	0	1	1	1	1	0	0	1	1	1	=	<table border="1" style="border-collapse: collapse; width: 100%; height: 100%;"> <tr><td>0</td><td>0</td><td>1</td><td>0</td><td>0</td></tr> <tr><td>0</td><td>1</td><td>1</td><td>1</td><td>0</td></tr> <tr><td>0</td><td>1</td><td>1</td><td>1</td><td>1</td></tr> <tr><td>0</td><td>1</td><td>1</td><td>0</td><td>0</td></tr> <tr><td>0</td><td>0</td><td>0</td><td>0</td><td>0</td></tr> </table>	0	0	1	0	0	0	1	1	1	0	0	1	1	1	1	0	1	1	0	0	0	0	0	0	0
0	1	1	0	0																																																																											
0	1	1	1	0																																																																											
0	1	1	1	1																																																																											
1	1	1	0	0																																																																											
0	0	0	0	0																																																																											
0	0	1	1	0																																																																											
0	1	1	1	0																																																																											
0	1	1	1	1																																																																											
0	1	1	1	1																																																																											
0	0	1	1	1																																																																											
0	0	1	0	0																																																																											
0	1	1	1	0																																																																											
0	1	1	1	1																																																																											
0	1	1	0	0																																																																											
0	0	0	0	0																																																																											
Pb_bool_sector1.mod		Zn_bool_sector1.mod		Pb_x_Zn_bool_sector1.mod																																																																											

Figure 6- Schematic representation of multiplication operation that are applied to the Boolean files belonging to Sector 1 (the numbers were arbitrarily selected) (Akıška et al., 2013).

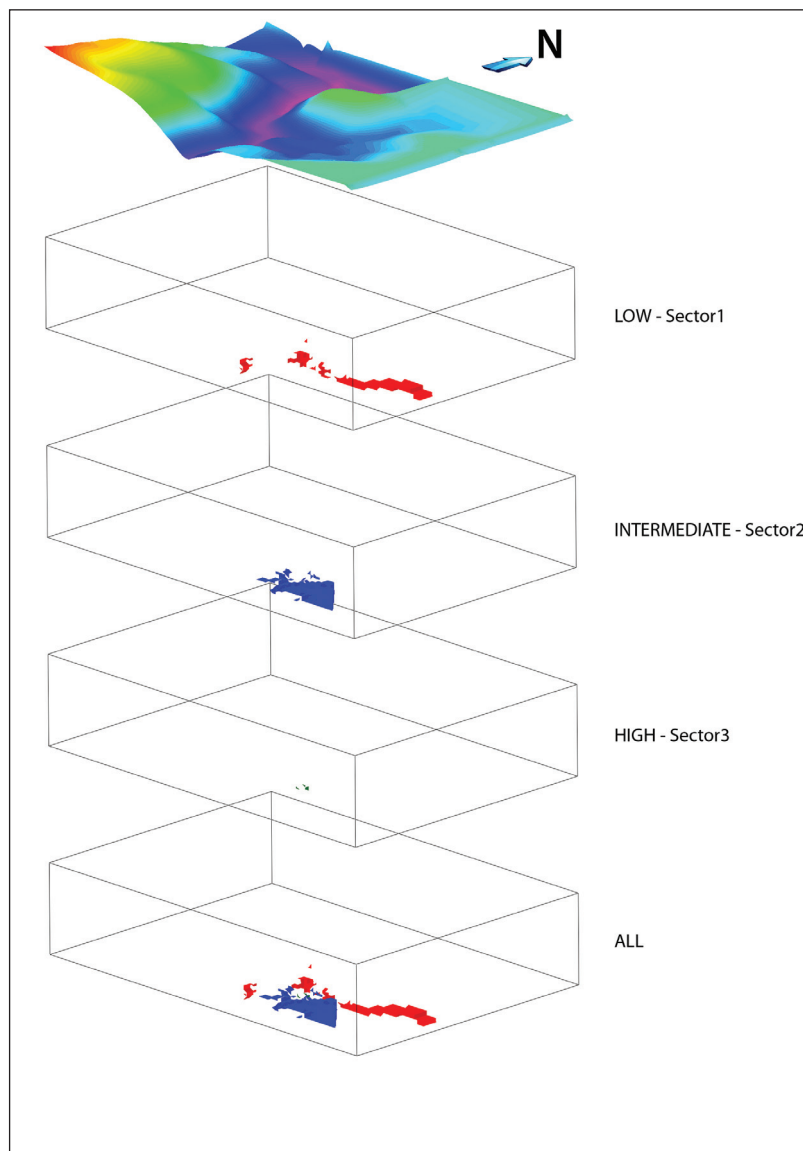


Figure 7- The subsurface locations of the sectors of Pb% and Zn% values above the cut-off grade.

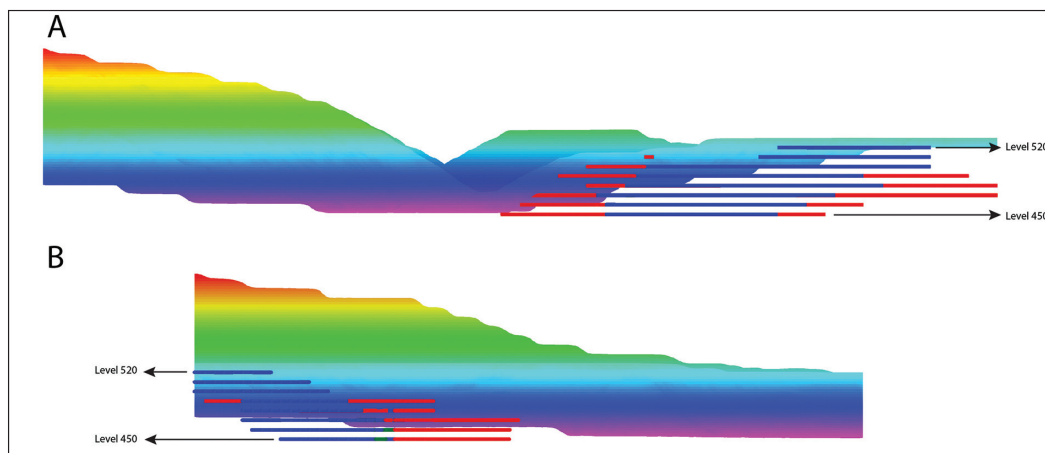


Figure 8- The southern (a) and the eastern (b) views of the adits obtained as a result of modeling study and the intersecting areas of sector groups (See figure 7 for the color of sector areas).

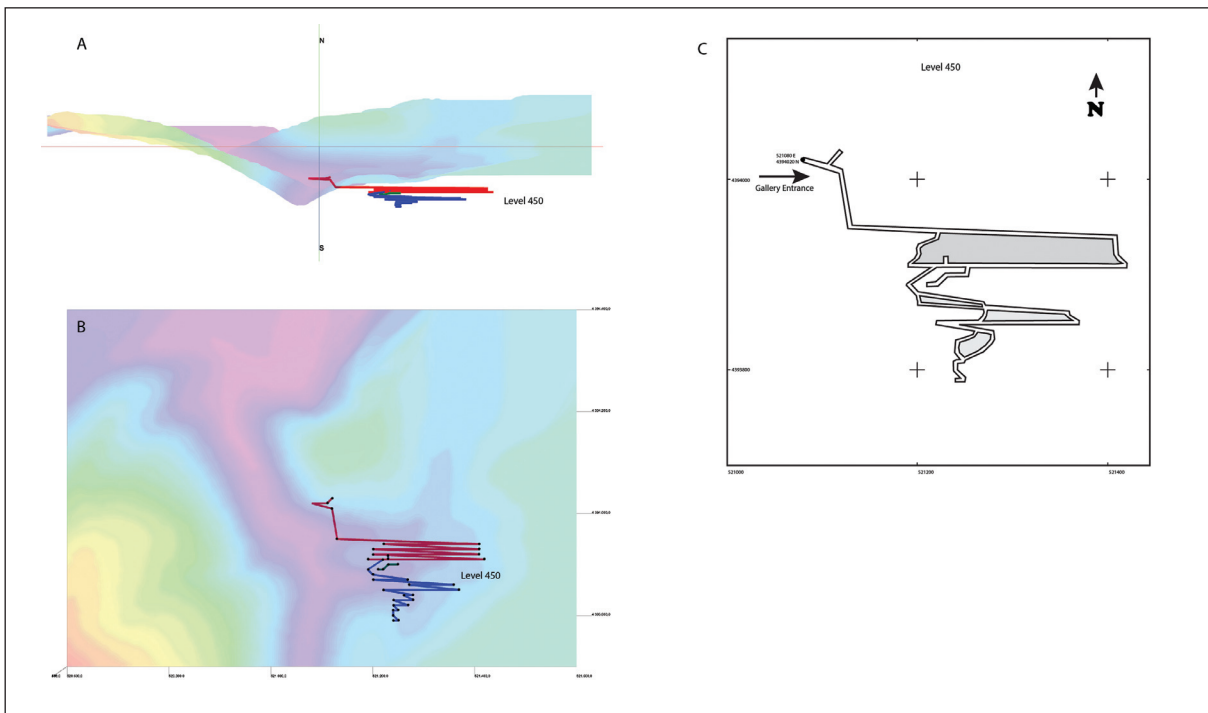


Figure 9- A) 3D topographic map and the sample adit line at Level 450 (the opacity value of the 3D topographic map has been reduced to 30% and the angle of view has been tilted 13° to the top along the x axis) (side of view: from South) (see figure 4 for the legend of the topographic elevations and figure 7 for the explanations of the sector colors), B) Side of view: from Top, C) Interpreted adit map of 450 level.

Table 3- Prediction errors of modeling study using IDW method.

		%Pb	%Zn
Samples	n	7170	7170
Mean Error	ME	0.00011	0.00023
Root-Mean-Square Error	RMSE	1.02861	0.56252

5. Conclusions

The surface modeling study using Kriging method and the subsurface modeling study using IDW method are intended to show the spatial trends and variability of the ore zones and also to determine the probable adit locations. For this purpose, to determine the appropriate adit lines the geochemical data and the location of the subsurface ore was used.

With the help of geostatistical analyses made on the topographic data used to create DEM, the suitable interpolation algorithm and the semi-variogram were determined and all results were controlled statistically and using cross-validation technique. As a result, the most suitable interpolation algorithm is “Ordinary Kriging” and the semi-variogram is “Spherical model”. The lag size is 52,72 m, sill value is 5396,57 m, and nugget value is 0 m. The suitable shape for

neighborhood estimation was determined as circle that have four sectors divided by 45° offset and the number of neighborhoods was between 2 and 5.

Pb% and Zn% values were detected with the help of geochemical analyses of the ore zones in the 42 surface and subsurface boreholes. The ore zones in the subsurface environment for Pb% and Zn% were determined using this data. From the detected areas, the parts above the cut-off grade were modeled. The large areas were specified as a result of this modeling study. It is not appropriate to use this data directly because of the limited number of boreholes, whose distances were not regularly spaced, and because the boreholes were not regularly distributed over the whole study area. Instead, the areas above the cut-off grades for both Pb% and Zn% were divided into 4 sectors to identify more specific areas (low, intermediate, high, very high). Then, the intersection areas in the subsurface environment of the same sectors for Pb% and Zn% were specified and an attempt to determine the appropriate adit lines was tried. The IDW interpolation algorithm was used for the modeling of subsurface data. The power and the neighborhood values were tested for both Pb% and Zn% values and the optimal values are; power value 8

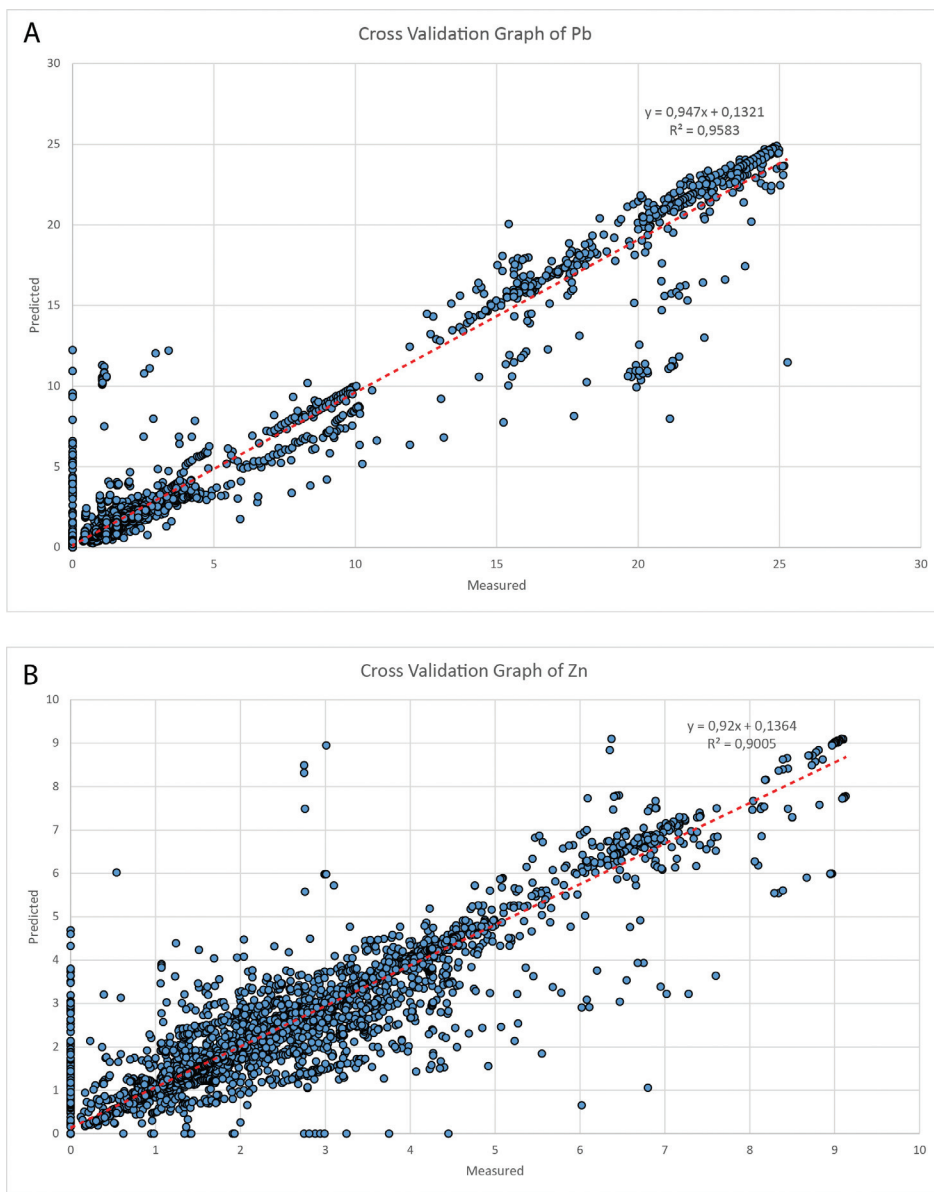


Figure 10- Cross-validation graph of the measured-estimated values of Pb% and Zn%.

and number of neighborhoods 6 for Pb%, power value 4 and number of neighborhoods 2 for Zn%.

The cross-validation results and the prediction errors obtained from the surface modeling study are shown in figure 3 and table 1, respectively, while the cross-validation results and the prediction errors obtained from the subsurface modeling study are shown in figure 10 and table 3, respectively. In this study, the modeling studies are evaluated considering all the data and the results obtained from the modeling studies are presented taking these values into consideration.

The number of sectors and the sector intervals were determined randomly in this study. These features may show changes in each different area. The sector intervals may be determined based on deposit conditions, economic conditions, and metal prices etc. Generally, modeling studies are carried out before the mining operations and the ore zones are operated in the frame of the model. However, depending on the importance of changes in the conditions on that day (e.g. sudden increases and decreases in costs, changes in metal prices), these models can be regenerated or the sector intervals on the created model can be changed. In this way, a model that can be actively used and can be changed during the mining operations is presented

in this study. Although all the modeling studies up to this point were controlled by the geostatistical and cross-validation methods, the geological data such as lithology, the general position of ore, and structural elements should always be prioritized.

Acknowledgements

The authors would like to thank Oreks Madencilik for providing the data for this study and for granting permission to study on the field.

References

- Ahlberg, J., Nilson, E., Walsh, J. 1967. The Theory of Splines and its Applications. Academic Press, New York, 280 p.
- Ahmed, A.A. 2009. Using lithologic modeling techniques for aquifer characterization and groundwater flow modeling of the Sohag area, Egypt. *Hydrogeology Journal* 17, 1189–1201.
- Akışka, S. 2010. Yenice (Çanakkale) Bölgesi'ndeki Cu-Pb-Zn Oluşumları. Doktora Tezi, Ankara Üniversitesi, 234 s. Ankara (unpublished).
- Akışka, S., Demirela, G., Sayılı, İ.S., Kuşcu, İ. 2010. Fluid inclusion and S isotope systematics of some carbonate-related Pb-Zn-Cu mineralizations in NW Anatolia, Turkey. Melfos, V., Marchev, P., Lakova, I., Chatzipetros, A. (Ed). *Geologica Balcanica Abstract Volume*, 21.
- Akışka, S., Sayılı, İ.S., Demirela, G. 2013. 3D Subsurface Modeling of Mineralization: A Case Study from Haderesi (Çanakkale, NW Turkey) Pb-Zn-Cu Deposit. *Turkish Journal of Earth Sciences* 22, 574-587.
- Akışka, S., Demirela, G. 2014. Haderesi, Bağırkaçdere ve Firincıkdere (Kalkım, Yenice - ÇANAKKALE) Pb-Zn±Cu Distal Skarn Yataklarında Akışkanların Kökeni. *Yerbilimleri* 35(3):, 199-218.
- Altunkaynak, Ş., Genç, Ş.C. 2008. Petrogenesis and time-progressive evolution of the Cenozoic continental volcanism in the Biga Peninsula, NWAnatolia (Turkey). *Lithos* 102, 316-340.
- Andiç, T., Kayhan, F. 1996. Havran-İvrindi (Balıkesir), Kalkım-Pazarköy (Çanakkale) yöresinde yapılmış genel ve tahlük jeokimya çalışma raporu, Maden Tetkik ve Arama Genel Müdürlüğü Rapor No: 9900, Ankara (unpublished).
- Binh, T.Q., Thuy, N.T. 2008. Assessment of the influence of interpolation techniques on the accuracy of digital elevation model. *VNU Journal of Science, Earth Sciences* 24, 176–183.
- Bistacchi, A., Massironi, M., Dal Piaz, G.V., Dal Piaz, G., Monopoli, B., Schiavo, A., Toffolon, G. 2008. 3D fold and fault reconstruction with uncertainty model: an example from an Alpine tunnel case study. *Computers & Geosciences* 34, 351–372.
- Brooker, P.I. 1986. A parametric study of robustness of kriging variance as a function of range and relative nugget effect for a spherical semivariogram. *Mathematical Geology* 18, 477–488.
- Burrough, P.A., McDonnell, R.A. 1998. Principles of Geographical Information Systems. Oxford University Press, 356 p.
- Calcagno, P., Chilès, J.P., Courrioux, G., Guillen, A. 2008. Geological modelling from field data and geological knowledge Part I. Modelling method coupling 3D potential-field interpolation and geological rules. *Physics of the Earth and Planetary Interiors* 171, 147–157.
- Chauouai, N.E., Fytas, K. 1991. A sensitivity analysis of search distance and number of samples in indicator kriging. *CIM Bulletin* 84, 37–43.
- Chaplot, V., Darboux, F., Bourennane, H., Leguedois, S., Silvera, N., Phachomphon, K. 2006. Accuracy of interpolation techniques for the derivation of digital elevation models in relation to landform types and data density. *Geomorphology* 77, 126–141.
- Chen, J., Lu, P., Wu, W., Zhao, J., Hu, Q. 2007. A 3-D Prediction Method for Blind Orebody Based on 3-D Visualization Model and Its Application. *Earth Science Frontiers* 14(5), 54-62.
- Choi, Y., Yoon, S.-Y., Park, H.-D. 2009. Tunneling Analyst: a 3D GIS extension for rock mass classification and fault zone analysis in tunneling. *Computers & Geosciences* 35, 1322–1333.
- Cressie, N.A.C. 1990. The origins of kriging. *Mathematical Geology* 22, 239–252.
- Çetinkaya, N., Karul, B., Önal, R., Yenigün, K. 1983a. Çanakkale-Yenice-Kalkım Bağırkaç Dere jeoloji raporu. Maden Tetkik ve Arama Genel Müdürlüğü Rapor No: 7814, Ankara (unpublished).
- Çetinkaya, N., Karul, B., Önal, R., Yenigün, K. 1983b. Çanakkale-Yenice-Kalkım Haderesi Pb-Zn-Cu yatağı jeoloji raporu. Maden Tetkik ve Arama Genel Müdürlüğü Rapor No:7822, Ankara (unpublished).
- Dağ A., Özdemir A.C. 2013. A Comparative Study for 3D Surface Modeling of Coal Deposit by Spatial Interpolation Approaches, *Resource Geology* 63, 394-403.

- Davis, B.M. 1987. Uses and abuses of cross-validation in geostatistics. *Mathematical Geology* 19, 241–248.
- de Kemp, E.A. 2000. 3-D visualization of structural field data: examples from the Archean Caopatina Formation, Abitibi greenstone belt, Québec, Canada. *Computers & Geosciences* 26, 509–530.
- Dhont, D., Monod, B., Hervouët, Y., Backé, G., Klarica, S., Choy, J.E. 2012. 3D geological modeling of the Trujillo block: Insights for crustal escape models of the Venezuelan Andes. *Journal of South American Earth Sciences* 39, 245–251.
- Dilek, Y., Altunkaynak, S., Öner, Z. 2009. Syn-extensional granitoids in the Menderes core complex, and the late Cenozoic extensional tectonics of the Aegean province. *Geological Society of London, Special Publications* 321, 197–223.
- Dönmez, M., Akçay, A.E., Genç, S.C., Acar, S. 2005. Biga Yarımadası'nda Orta-Üst Eosen volkanizması ve denizel ignimbritler. *Maden Tetkik ve Arama Genel Müdürlüğü Dergisi* 131, 49–61.
- Dönmez, M., Akçay, A.E., Duru, M., İlgar, A., Pehlivan, S. 2008. Türkiye Jeoloji Haritaları Çanakkale-H17 Paftası. *Maden Tetkik ve Arama Genel Müdürlüğü Jeoloji Etütleri Dairesi*, 101 s.
- Dressler, M. 2009. Art of Surface Interpolation. Doktora Tezi, Technical University of Liberec, 80p. Liberec (unpublished).
- Duru, M., Pehlivan, S., Dönmez, M., İlgar, A. Akçay, A.E. 2007. Balıkesir İ18 paftasının Jeolojik Haritası. *Maden Tetkik ve Arama Genel Müdürlüğü Rapor No: 97*, Ankara (unpublished).
- Elkadi, A.S., Huisman, M. 2002. 3D-GSIS geotechnical modeling of tunnel intersection in soft ground: the second Heinenoord tunnel, Netherlands. *Tunnelling and Underground Space Technology* 17, 363–369.
- Falivene, O., Cabrera, L., Tolosana-Delgado, R., Alberto, S. 2010. Interpolation algorithm ranking using cross-validation and the role of smoothing effect. A coal zone example. *Computers & Geosciences* 36, 512–519.
- Feltrin, L., McLellan, J.G., Oliver, N.H.S. 2009. Modelling the giant, Zn-Pb-Ag century deposit, Queensland, Australia. *Computers & Geosciences* 35, 108–133.
- Fencík, R., Vajsálová, M. 2006. Parameters of interpolation methods of creation of digital model of landscape. The 9th AGILE Conference on Geographic Information Science, 2006, Visegrad, Hungary, 374–381.
- Galera, C., Tennen, C., Moretti, I., Mallet, J.L. 2003. Construction of coherent 3D geological blocks. *Computers & Geosciences* 29, 971–984.
- Gallerini, G., De Donatis, M. 2009. 3D modeling using geognostic data: The case of the low valley of Foglia river (Italy): *Computers & Geosciences* 35, 146–164.
- Genç, S.C., Altunkaynak, S. 2007. Eybek graniti (Biga yarımadası, KB Anadolu) üzerine: Yeni jeokimya verileri ışığında yeni bir değerlendirme. *Yerbilimleri*, 28(2), 75–98.
- Hack, R., Orlic, B., Özmutlu, S., Zhu, S., Rengers, N. 2006. Three and more dimensional modelling in geo-engineering. *Bulletin of Engineering Geology and the Environment* 65, 143–153.
- Hu, K., Li, B., Lu, Y., Zhang, F. 2004. Comparison of various spatial interpolation methods for non-stationary regional soil mercury content. *Environmental Science* 25(3), 132–137.
- Isaaks, E.H., Srivastava, R.M. 1989. *Applied Geostatistics*. Oxford University Press, New York, 561 p.
- Jian, W., Yuanhui, S., Bin, W., Yongjun, W., Lei, X., Chunmeng, D. 2012. 3D geological modeling of fractured volcanic reservoir bodies in Block DX18 in Junggar Basin, NW China. *Petroleum Exploration and Development* 39(1), 99–106.
- Johnston, K., Ver Hoef, J.M., Krivoruchko, K., Lucas, N. 2001. *Using ArcGIS Geostatistical Analyst*. ESRI Press Redlands, CA, USA, 300 p.
- Kane, V.E., Begovich, C.L., Butz, T.R., Myers, D. 1982. Interpretation of regional geochemistry using optimal interpolation parameters. *Computers & Geosciences* 8 (2), 117–135.
- Kashani, S.B.M., Abedi, M., Norouzi, G.H. 2016. Fuzzy logic mineral potential mapping for copper exploration using multi-disciplinary geo-datasets, a case study in seridune deposit, Iran. *Earth Science Informatics* 9, 167–181.
- Kaufmann, O., Martin, T. 2008. 3D geological modelling from boreholes, cross-sections and geological maps, application over former natural gas storages in coal mines. *Computers & Geosciences* 34, 278–290.
- Kitanidis, P.K. 1997. *Introduction to Geostatistics: Applications in Hydrogeology*. Cambridge University Press, Cambridge, USA, 249 p.
- Krigie, D.G. 1951. A statistical approach to some basic mine valuation problems on the Witwatersrand. *Journal of the Chemical, Metallurgical and Mining Society of South Africa* 52, 119–139.

- Krushensky, R.D. 1976. Neogene calc-alkaline extrusive and intrusive rocks of the Karalar-Yeşiller area, Northwest Anatolia. *Bulletin Volcanologique* 39, 336–360.
- Lam, N.S. 1983. Spatial interpolation methods review. *The American Cartographer* 10, 129–149.
- Li, J., Heap, A. 2008. A Review of Spatial Interpolation Methods for Environmental Scientists. *Geoscience Australia Record/23*, 137p.
- Liu, L., Zhao, Y., Sun, T. 2012. 3D computational shape- and cooling process-modeling of magmatic intrusion and its implication for genesis and exploration of intrusion-related ore deposits: An example from the Yueshan intrusion in Anqing, China. *Tectonophysics* 526-529, 110-123.
- Matheron, G. 1960. Krigeage d'un Panneau Rectangulaire par sa Périphérie. *Note Geostatistique No. 28*, CG. Ecole des Mines de Paris, Paris.
- Mitasova, H., Mitas, L. 1993. Interpolation by Regularized Spline with Tension: I. Theory and Implementation. *Mathematical Geology* 25, 641-655.
- Okay, A.İ., Siyako, M., Bürkan, K.A. 1990. Biga Yarımadası'nın jeolojisi ve tektonik evrimi. *Türkiye Petrol Jeoglari Derneği Bülteni* 2, 83–121.
- Okay, A.İ., Satır, M., Maluski, H., Siyako, M., Monie, P., Metzger, R., Akyüz S. 1996. Paleo- and Neo-Tethyan events in northwest Turkey: geological and geochronological constraints. Yin, A., Harrison, M. (Ed.). *Tectonics of Asia*. Cambridge University Press, Cambridge, 420–441.
- Okay, A.İ., Bozkurt, E., Satır, M., Yiğitbaş, E., Crowley, Q.G., Cosmas, K.S. 2008. Defining the southern margin of Avalonia in the Pontides: Geochronological data from the Late Proterozoic and Ordovician granitoids from NW Turkey. *Tectonophysics* 461, 252-264.
- Olea, R.A. 1999. *Geostatistics for Engineers and Earth Scientists*. Kluwer Academic Publishers, London, UK, 303 p.
- Özmutlu, S., Hack, R. 2003. 3D modelling system for ground engineering. Rosenbaum, M.S., Turner, A.K. (Ed.). *New Paradigms in Subsurface Prediction Characterization of the Shallow Subsurface Implications for Urban Infrastructure and Environmental Assessment*, Lecture Notes in Earth Sciences 99, 253–260.
- Pehlivan, A.N., Çetin, A. 1997. Edremit (Balikesir) Ezine-Bayramiç-Yenice (Çanakkale) çevresinin altın açısından polimetal ve ağır mineral çalışmaları raporu. Maden Tetkik ve Arama Genel Müdürlüğü Rapor No: 10061, Ankara (unpublished).
- Peralvo, M. 2004. Influence of DEM interpolation methods in drainage analysis. *GIS Hydro 04*, University of Texas, Austin, Texas, 26 p.
- Radelli, L. 1970. La nappe de Balya la zone plis Egéenne et extension de la zone du Vardar en Turquie occidentale. *Géologie Alpine* 46, 169-175.
- Renard, P., Courrioux, G. 1994. Three-dimensional geometric modeling of a faulted domain: the Soultz Horst example (Alsace, France). *Computers & Geosciences* 20, 1379–1390.
- Rengers, N., Hack, R., Huisman, M., Slob S., Zigterman, W. 2002. Information technology applied to engineering geology. van Rooy, J.L., Jermy, C.A. (Ed.). *Engineering Geology for Developing Countries – Proceedings of 9th Congress of the International Association for Engineering Geology and the Environment*, 121–143.
- Robinson, T.P., Metternicht, G. 2006. Testing the performance of spatial interpolation techniques for mapping soil properties. *Computers and Electronics in Agriculture* 50, 97-108.
- Saraç, C., Tercan, A.E. 1996. Grade and reserve estimation of the Tulovasi borate deposit by block kriging. *International Geology Review* 38, 832–837.
- Saraç, C., Demirel, I.H., Sen, O., Varol, N. 2004. Geostatistical Simulation of the Total Organic Carbon Values: An Example from Petroleum Source Rocks on the Coastal Area of Western Taurus Region, Turkey. *Petroleum Science and Technology* 22(3&4), 367-379.
- Shahbeik, S., Afzal, P., Moarefvand, P., Qumarsy, M. 2014. Comparison between Ordinary Kriging (OK) and Inverse Distance Weighted (IDW) based on estimation error Case study: in Dardevey iron ore deposit, NE Iran. *Arabian Journal of Geosciences* 7, 3693–3704.
- Sims, D.L. 1992. Application of 3D geoscientific modelling for hydrocarbon exploration. Turner, A.K. (Ed.) *Three-Dimensional Modelling with Geoscientific Information systems*, Kluwer Academic Publishers, 443 p.
- Siyako, M., Bürkan, K.A., Okay, İ.A. 1989. Biga ve Gelibolu Yarımadası'nın Tersiyer jeolojisi ve hidrokarbon olanakları. *Türkiye Petrol Jeoglari Derneği Bülteni* 1(3), 183-199.
- Tahmasebi, P., Hezarkhani, A. 2010. Application of adaptive neuro-fuzzy inference system for grade estimation; case study, Sarcheshmeh porphyry copper deposit, Kerman, Iran. *Australian Journal of Basic and Applied Sciences* 4, 408–420.

- Tufan, A.E. 1993. Karaydin Köyü (Yenice-Çanakkale) çevresinin jeolojik ve petrografik özelliklerini ile kurşun-çinko zuhurlarının jenetik incelemesi. Doktora Tezi, Selçuk Üniversitesi, 158 s. Konya (unpublished).
- Turner, A. K. 1992. Three- Dimensional Modelling with Geo-scientific Information Systems. Kluwer Academic Publishers, 468 p.
- Van Dijk, M.J., Rientjes, T.H.M., Boekelman, R.H. 1999. Interpolation schemes, H.P., Bähr and T., Vögtle (Ed.). GIS for Environmental Monitoring. Schweizerbart 183 - 189.
- Veldkamp, J.G., Hack, H.R.G.K., Özmutlu, S., Hendriks M.A.N., Kronieger, R., Van Deen, J.K. 2001. Combination of 3D-GIS and FEM modelling of the 2nd Heinenoord Tunnel, The Netherlands. Abstract to the International Symposium, EngGeoCity – 2001 ‘Engineering Geological Problems of Urban Areas’, 30 July-2 August 2001, Ekaterinburg, Russia, 1-8.
- Voltz, M., Webster, R. 1990. A comparison of kriging, cubic splines and classification for predicting soil properties from sample information. European Journal of Soil Science 41, 473–490.
- Wang, G., Huang, L. 2012. 3D geological modeling for mineral resource assessment of the Tongshan Cu deposit, Heilongjiang Province, China. Geoscience Frontiers 3, 483-491.
- Wang, G., Zhang, S., Yan, C., Song, Y., Sun, Y., Li, D., Xu, F. 2011. Mineral potential targeting and resource assessment based on 3D geological modeling in Luanchuan region, China. Computers & Geosciences 37, 1976–1988.
- Watt, J.T., Glen, J.M.G., John, D.A., Ponce, D.A. 2007. Three-dimensional geologic model of the northern Nevada rift and the Beowawe geothermal system, north-central Nevada. Geosphere 3(6), 667–682.
- Webster, R., Oliver, M.A. 2001. Geostatistics for Environmental Scientists. John Wiley and Sons, 360 p.
- Xiao, F., Chen, J., Zhang, Z., Wang, C., Wu, G., Agterberg, F.P. 2012. Singularity mapping and spatially weighted principal component analysis to identify geochemical anomalies associated with Ag and Pb-Zn polymetallic mineralization in Northwest Zhejiang, China. Journal of Geochemical Exploration 122, 90–100.
- Yücelay, M.A. 1975. Çanakkale İli Yenice İlçesi Kalkım Bucağı Güneyindeki Çulfa Çukuru Kurşun Çinko Mineralizasyonu Jeolojik Etüdü, Maden Tetskik ve Arama Genel Müdürlüğü Rapor No: 5617, Ankara (unpublished).
- Yücelay, M.A. 1976. Çanakkale-Kalkım-Handeresi Pb-Zn-Cu bölgesinin etüdü. Maden Teskik ve Arama Genel Müdürlüğü Rapor No: 5720, Ankara (unpublished).
- Zanchi, A., Francesca, S., Stefano, Z., Simone, S., Graziano, G. 2009. 3D reconstruction of complex geological bodies: Examples from the Alps. Computers & Geosciences 35, 49-69.
- Zhu, S., Hack, R., Turner, A. K., Hale, M. 2003. How far will uncertainty of the subsurface limit the sustainability planning of the subsurface? Proceedings of Sustainable Development & Management of the Subsurface (SDMS) Conference, 5-7 Nov 2003, Utrecht, Netherlands. 203-210.
- Zimmerman, D., Pavlik, C., Ruggles, A., Armstrong, P. 1999. An experimental comparison of ordinary and universal kriging and inverse distance weighting. Mathematical Geology 31, 375–390.